Chapter

Spark Plasma Sintering of NiCrSiBC Alloys

Escarlet Batista da Silva, Márcia Giardinieri Azevedo, Lioudmila Aleksandrovna Matlakhova, Bárbara Ferreira de Oliveira and Luciano José de Oliveira

Abstract

Nickel-based alloys of the NiCrSiBC system (colmonoy alloys) are normally deposited on stainless-steel substrates for coating applications, once they present high resistance to wear and corrosion at high temperatures. Typically, deposition occurs through welding processes, such as PTA (plasma transferred arc) or laser cladding. This study mainly aims to evaluate the effectiveness of the spark plasma sintering (SPS) process through the evaluation of the sintered body density, and structural and microstructural analysis of the Colmonoy-5. SPS sintering occurred at 900°C under 50 MPa for 15 minutes. Powder morphology was evaluated by confocal microscopy. The sintered samples were evaluated according to their density (Archimedes' method), phase composition, microstructure, and hardness (Vickers hardness). Results showed that the Colmonoy-5 alloy can be effectively produced through SPS sintering, reaching densification above 90%. Microstructural analysis showed that there was the formation of hardening phases, such as borides and chromium carbides. The same phases are found in colmonoy alloys deposited on the stainless-steel substrate.

Keywords: colmonoy, sintering, spark plasma sintering, microstructure, vickers hardness

1. Introduction

Nickel-based alloys are widely used in various areas of industry, such as chemical, petrochemical, nuclear reactors, warfare, aerospace, food processing devices, and steel production facilities, due to an association of high mechanical strength, good corrosion resistance, and weldability. The performance of these alloys is associated with the face-centered cubic structure of the matrix, which can be hardened by solid solution or by precipitation of intermetallic compounds [1].

There are several hard-facing alloys, the most common of which are Fe-based, Co-based, and Ni-based. Co-based hard alloys have many applications, but they become radioactive in nuclear environments, and this phenomenon has restricted the use of Co-based coatings for high-temperature applications. To minimize workers' exposure to Co_{60} radiation during handling and maintenance operations, nickel-based hard-facing alloys from the NiCrSiBC family were developed. Colmonoy alloys (NiCrSiBC) have a wide variety of compositions and this consequently makes their use very abundant. It can be said that currently alloys are used preferentially for coating materials [2, 3].

It can be said that Ni-based hard-facing alloys, which still have carbides and borides in their structure formed from alloying elements, are popularly used as coating materials. Among the hard Ni-based alloys, colmonoy can be highlighted, which is widely used, and may also have different NiCrSiBC compositions depending on the alloying elements [4, 5].

Alloys from the NiCrSiBC family, such as colmonoy, have as their main characteristic their high resistance to wear and corrosion at high temperatures. These alloys were basically developed for deposition using some welding processes. Due to their excellent characteristics and lower cost compared to Co superalloys, Ni-based alloys have been deposited by various welding processes, such as plasma transferred arc (PTA), tungsten inert gas (TIG) and laser cladding [6–8].

The strength of colmonoy alloys (NiCrSiBC) can be increased by the formation of precipitates such as borides and carbides. Some studies of the alloys of the NiCrSiBC family deposited by laser cladding on a steel substrate showed the presence predominantly of the intermediate phases formed, in the form of carbides, borides, and silicides: CrB, Cr5B3, Ni4B3, Cr5B3, Cr7C3, and Ni3Si [9, 10].

Although welding deposition processes are widely used and applied, the substrate, which is usually stainless steel, has a high iron content, which can change the composition of the coating, causing the phenomenon known as dilution. The alloys of the NiCrSiBC family are very sensitive to the presence of the iron element, which results in a change in their microstructure and consequently in some mechanical properties, as observed in the works [9, 11, 12].

It should be noted that pulsed plasma sintering (SPS) can also be a processing route for nickel-based alloys, although still little explored, as mentioned in the work by [13]. In addition, there are no reports that clearly show the study of the influence of Fe on SPS-processed Ni-based alloys.

Spark plasma sintering is considered a powder metallurgy technique that features fast manufacturing routes at relatively low temperatures, involving simultaneous applications of pressure and temperature, resulting in engineering components with relatively high density and good mechanical properties, compared to others. Conventional sintering methods [14].

SPS technique stands out for its ease of operation and precision in sintering energy control, high sintering speeds, safety, and reliability [15].

Spark plasma sintering involves the simultaneous application of load as well as heat on the materials to be sintered. SPS is a new method meant for consolidation of nano-structured materials with hindered grain growth, efficient shrinkage in less time, and cleaner grain boundaries for effective interface formation. This technique utilizes high-temperature spark plasma generated by discharging exactly at the gaps of powder particles with an on-off electrical current. At the initial stage of the SPS process, the generated spark plasma induces neck formation and thermal diffusion process on the particles to be sintered. An electric field formed by DC current can also facilitate thermal diffusion process. Therefore, the SPS process involves the densification of poorly sinterable materials at a very short interval of time and at low temperature when compared with the conventional sintering process [16].

Colmonoy alloy properties are strongly related to the microstructure formed after alloy processing. Thus, in this work, greater attention was given to the correlation of the microstructural aspect and some important properties, such as density and hardness of colmonoy alloy, sintered by SPS, maintaining the parameters determined in the work of [5].

Currently, it can be said that there are few published works that report microstructural aspects of SPS-sintered NiCrSiBC alloys. Thus, the current literature basically brings studies of these alloys deposited on steel substrates, which often analyze the effect of Fe dilution on the microstructure of the alloy [17]. In this way, this work intends to show that it is possible to sinter the colmonoy alloy by the spark plasma sintering (SPS) process, and consequently contribute to future studies on the possibility of sintering the colmonoy alloy on a stainless-steel substrate.

2. Methodology

Commercial powders of Colmonoy-5 alloy (Ni-14Cr-3Si-2.5B-0.6C-4,2Fe) produced by the manufacturer WallColmonoy Corporation were used to process the samples. Powders were produced by atomization technique. The atomization process consists of casting system, which performs the fusion raw material for one induction oven under controlled environment where alloys are smelted, refined, and degassed. Refined melt metal is poured through a system crucible in a gas nozzle, where the stream of the melted metal beam is disintegrated from the kinetic energy of high-pressure inert gas flow (Argon). **Figure 1** shows a schematic of the gas atomization technique [18].

The average particle size of the powders was provided by the manufacturer. To analyze the morphology of the powders, images were made via confocal microscopy.

Colmonoy-5 alloys were sintered by spark plasma sintering (SPS) technique, maintaining technological parameters predetermined in the work [5]. SPS sintering occurred at 900°C under 50 MPa for 15 minutes.

The sintered material was subsequently characterized under structural aspects, microstructural, relative density, and Vickers hardness. **Figure 2** shows the general and succinct roadmap of the main stages of the development of the work.

In order to evaluate sintering effectiveness, the densification alloy after sintering was measured. For that, the density (apparent specific gravity) was determined using the Archimedes method, using four samples. The calculation of the apparent specific mass is based on the value of the dry mass of the sintered (MS), the mass of the same immersed in water (MI), and the saturated mass (MA) that is obtained after the sample is boiled for a period of 20 minutes. For this, the density of water is also considered, as shown in eq. 1. The percentage of densification (relative density) was calculated from the values of the experimental density of the sintered material and the theoretical density (eq. 2), that is, it is the ratio between the ASG of the sample and theoretical alloy density of 8,14 g/cm^3 [4].

$$ASG = \frac{MS}{(MA - MI)}\, x\, \rho_{H2O} \tag{1}$$

$$Density(\%) = \frac{ASG}{Density\ Theorical}\, x\, 100 \tag{2}$$

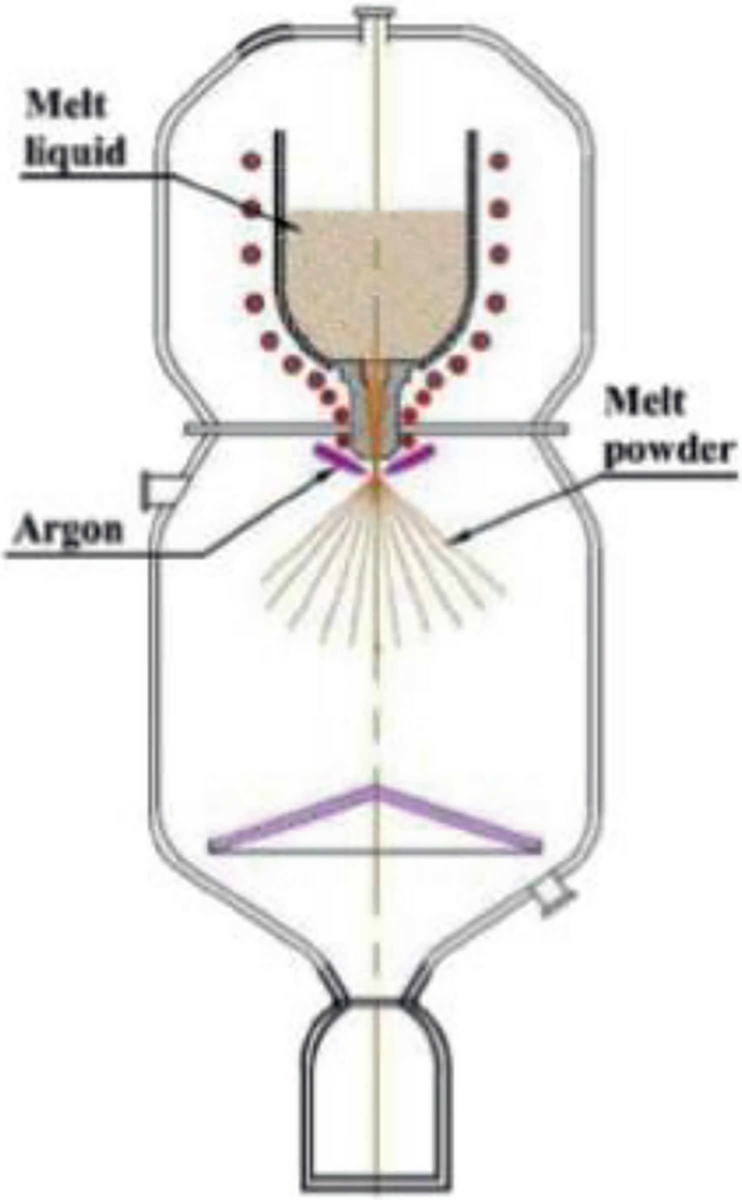

Figure 1.
Gas atomization process [18].

The microstructural aspect of the sintered body after SPS was performed from SEM. Before SEM analysis, the samples were metallographically prepared, first sanded (100 to 1200 mesh), and later polished and subjected to chemical attack. Phase identification was performed through X-ray diffraction analysis, using a Bruker D2 phaser diffractometer. The diffractometer is equipped with a Cu-Kα radiation tube, where the samples were scanned in the 2θ range, with an interval between 20° and 90°, under a step of 0.05° for 3 seconds. The characteristic peaks in the diffractions obtained were analyzed, and the results were compared with the ICDD (International Center Diffraction Data) database, to help identify the phases present.

Vickers hardness tests were carried out with the aid of a digital micro hardness tester DHT, HVS – 1000, performing five indentations [19, 20] in each sample and applying a load of 1 kgf in the tests for a time of 10 seconds.

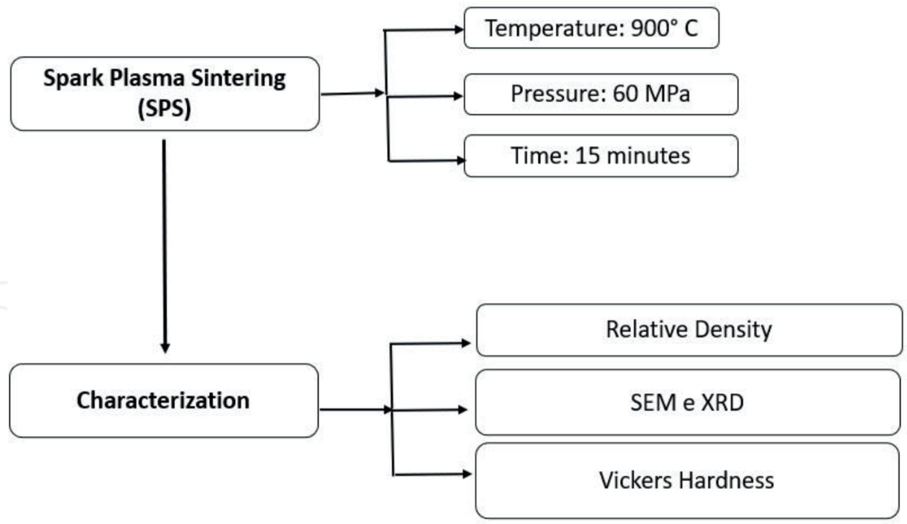

Figure 2.
Processing route, characterization steps, and testing of Colmonoy-5 alloy.

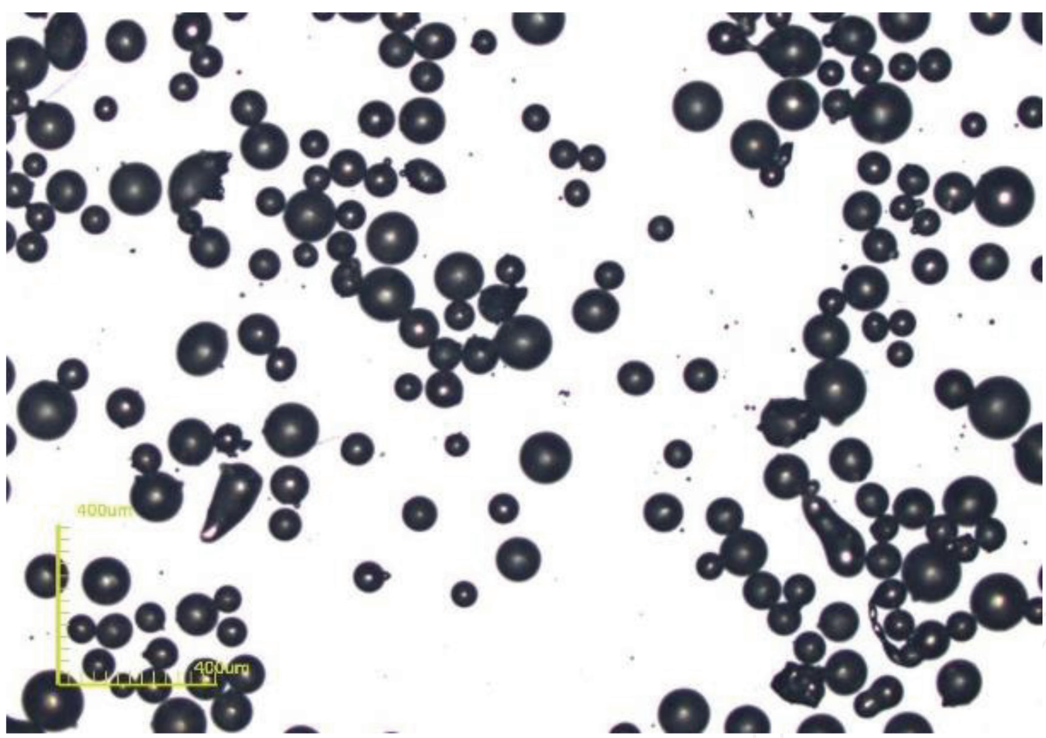

Figure 3.
Colmonoy-5 alloy powders with spherical morphology.

3. Results and discussion

Table 1 shows the mean values of the apparent specific gravity (ASG) measurements of the four samples, and their respective standard deviations. ASG values verified were around 7.5 g/cm^3 on average. Through eq. 2, it was obtained about 92% densification (ASG/theoretical density), indicating that SPS sintering was effective. Density may increase as a function of sintering temperature. Thus, it is believed that we can achieve densification greater than 92% at temperatures higher than those used in this study [19, 20].

Pressão (MPa)	MEA (g/cm^3)	DP
60	7.47	± 0.168

Table 1.
Apparent specific gravity (ASG) is calculated by the Archimedes method.

Figure 3 shows it is possible to observe regular shaped powder particles and predominantly spherical morphology, which is a common characteristic of powders produced by atomization and may also have contributed to the good densification achieved. Evaluation of the average size of the powders revealed an average size of 74 to 149 μm.

Figure 4 shows XRD Colmonoy-5 alloys sintered by SPS. In all sintered samples, in addition to nickel, the presence of several important phases, such as borides (CrB, Ni_2B, Cr_2B, Ni_3B, and Cr_5B_3), as well as Cr_7C_3 chromium carbide. The phases verified in the XRD analysis of the bodies sintered by SPS are the same obtained in the diffractograms of the initial powders, which is in perfect agreement with the works [11, 21, 22].

Figure 5 shows fine precipitated phases and homogeneous distribution. Chromium borides appear in the form of very fine dark modules and small dark blocks. Studies by Ref. [23] on NiCrSiBC alloys indicated in a transmission electron microscope (TEM) analysis that Cr_2B chromium boride can be presented in the form of small dark blocks. There is also an intense formation of laths and small blocks in half-ton (lighter phase) well distributed in the matrix phase, which is probably chromium carbide.

It can be seen in **Figure 6**(a), again the presence of chromium borides (dark phase) in the form of fine needles and some small blocks. Note also a lighter phase in the form of a butterfly or wing (see circles), which is a precipitated phase rich in chromium. The EDS mapping in these regions, as shown in **Figure 6**(b), shows a high concentration of chromium in such phases, which actually indicates that it is a chromium-rich precipitate, specifically a Cr5B3 chromium boride [10]. It should be

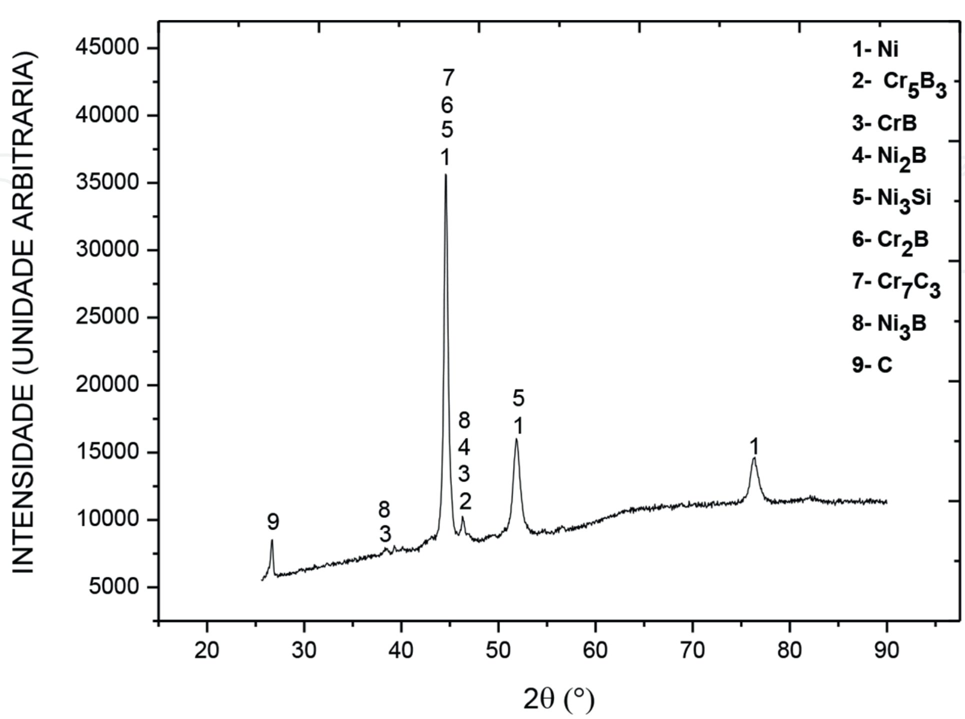

Figure 4.
XRD diffractograms of Colmonoy-5 alloys after SPS.

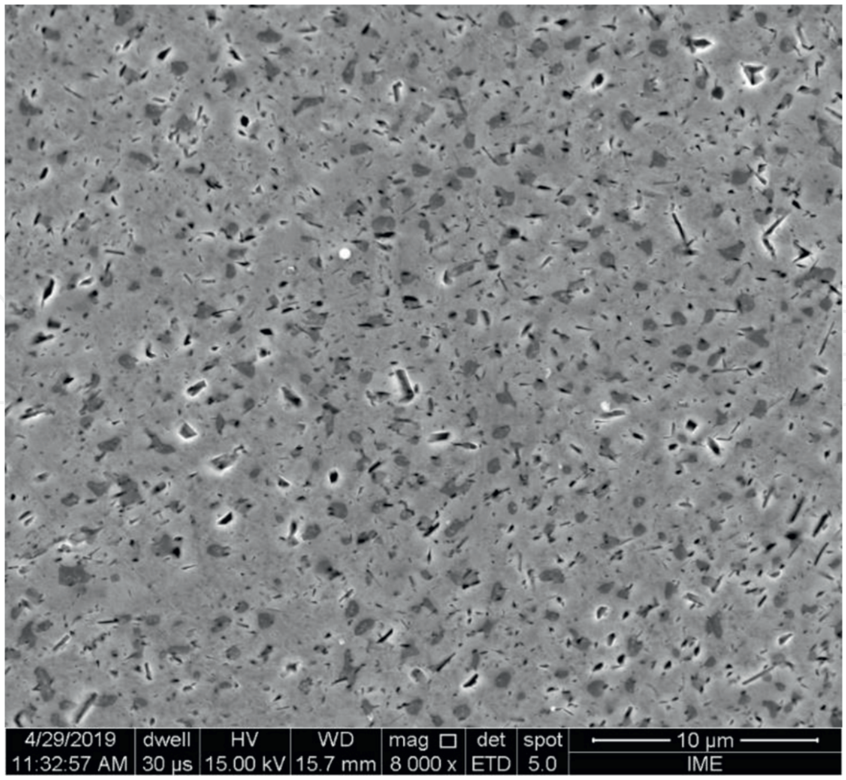

Figure 5.
Microstructure of Colmonoy-5 alloys sintered by SPS.

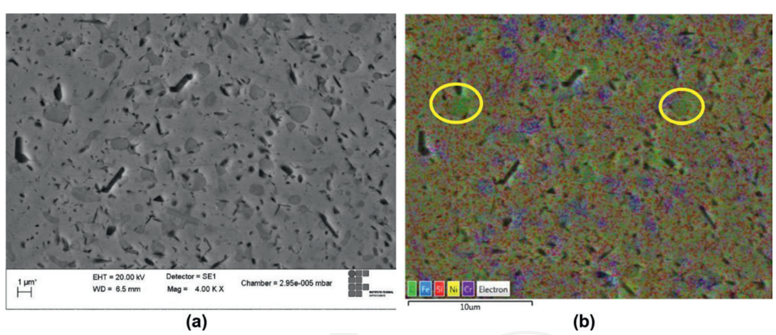

Figure 6.
(a) Microstructure and mapping region e (b) EDS image.

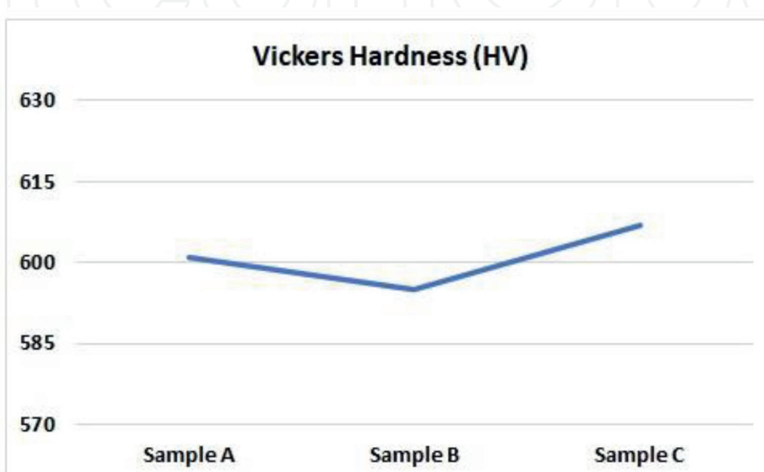

Figure 7.
Average hardness (HV) of the Colmonoy-5 alloy for 3 samples.

noted that it was not possible to capture boron element (B) by the EDS, due to the equipment limitation.

The average value obtained for the Vickers hardness of the Colmonoy-5 alloy sintered by SPS was 601 ± 6 HV, as shown in **Figure 7**. This result is in agreement with studies by Refs. [11, 12, 24].

4. Conclusion

The structural and microstructural analysis showed that phases formed after the SPS are the same as those found for the colmonoy alloy deposited.

The average hardness measured is within the range and in agreement with the literature in studies on colmonoy alloys.

It can be said that the SPS sintering of the Colmonoy-5 alloy was effective since it obtained densification above 90%. Thus, the SPS process can be a processing route for the colmonoy alloy.

Acknowledgements

The authors are grateful for the support of the Brazilian institutions FAPERJ, IME, and IFES campus Vitória/ES throughout the development of this study.

Author details

Escarlet Batista da Silva[1*], Márcia Giardinieri Azevedo[1], Lioudmila Aleksandrovna Matlakhova[1], Bárbara Ferreira de Oliveira[1] and Luciano José de Oliveira[2]

1 Advanced Materials Laboratory, CCT/UENF – State University of Northern Rio de Janeiro, Campos, RJ, Brazil

2 Institute of Society Science, MDM/UFF – Fluminense Federal University, Macaé, RJ, Brazil

*Address all correspondence to: escarletbatistadsilva@gmail.com

References

[1] Sandes SS et al. Avaliação de Revestimentos de Liga de Níquel 625 Depositados pelo Processo Eletroescória. Soldagem & Inspeção. 2016;**1**(4):417-427

[2] Das CR et al. Effects of dilution on microstructure and wear behaviour of NiCr hardface deposits. Materials Science and Technology. 2007;**23**(9):771-779

[3] Kumar H et al. Friction and wear behaviour of Ni-Cr-B hardface coating on 316LN stainless steel in liquid sodium at elevated temperature. Journal of Nuclear Materials. 2017;**495**:431-437

[4] Handbook ASM. ASM Specialty Handbook: Nickel, Cobalt, and their Alloys. In: Davis JR, editor. EUA. Davis & Associates; 2000

[5] Silva B. Caracterização da liga Colmonoy-5 sinterizada por plasma pulsado (SPS)", Dissertação (Mestrado em Engenharia e Ciência dos Materiais). Campos dos Goytacazes – RJ: Universidade Estadual do Norte Fluminense – UENF; 2019

[6] Luo JL et al. Effect of NiCrBSi contente on microstructural evolution, cracking susceptibility and wear behaviors of laser cladding WC/Ni-NiCrBSi composite coatings. Journal of Alloys and Compounds. 2015;**626**:102-111

[7] Benea L et al. Fretting and wear behaviors of Ni/nano-WC composite coatings in dry and wet conditions. Materials and Design. 2015;**65**:550-558

[8] Araújo PHD. Caracterização de Materiais Dissimilares com Revestimentos NiCrSiBC em Diferentes Substratos", Dissertação (Mestrado em Engenharia e Ciência dos Materiais). Campos dos Goytacazes – RJ: Universidade Estadual do Norte Fluminense – UENF; 2016. p. 27

[9] Silva LJ, D'Oliveira ASC. Liga NiCrSiBC: Microestrutura e Dureza de Revestimentos Processados a Arco e a Laser. Soldagem & Inspeção. 2015;**20**(1):39-47

[10] Hemmati I et al. Effects of the alloy composition on phase constitution and properties of laser deposited Ni-Cr-B-Si coatings. Physics Procedia. 2013;**41**:302-311

[11] Hemmati et al. Dilution effects in laser cladding of Ni-Cr-B-Si-C hardfacing alloys. Materials Letters. 2012;**84**:69-72

[12] Silva LJ, D'Oliveira ASCM. NiCrSiBC coatings: Effect of dilution on microstructure and high temperature tribological behavior. Wear. 2016;**350-351**:130-140

[13] Yamanoglu R et al. Characterization of nickel alloy powders processed by spark plasma sintering. Powder Metallurgy. 2014;**57**(5):380-386

[14] Asl MS et al. Effects of sintering temperature on microstructure and mechanical properties of spark plasma sintered titanium. Materials Chemistry and Physics. 2018;**203**:266-273

[15] Borkar T, Banerjee R. Influence of spark plasma sintering (SPS) processing parameters on microstructure and mechanical properties of nickel. Materials Science & Engineering A. 2014;**618**:176-181

[16] Shashanka R et al. Effect of Y_2O_3 nanoparticles on corrosion study of spark plasma sintered duplex and ferritic stainless steel samples by linear sweep Voltammetric method.

Archives of Metallurgy and Materials. 2018;**63**(2):749-763

[17] Balaguru S, e Gupta, M. Hardfacing studies of No alloys: A critical review. Journal of Materials Research and Technology. 2021;**10**:1210-1242

[18] Chen G et al. A comparative study of Ti-6Al-4V powders for aditive manufacturing by gas atomization, plasma rotating electrode process and plasma atomization. Powder Technology. 2018;**333**:38-46

[19] Shashanka R, Chaira D. Effect of sintering temperature and atmosphere on nonlubricated sliding Wear of Nano-Yttria-dispersed and Yttria-free duplex and ferritic stainless steel. Tribology Transactions. 2017;**60**(2):324-336

[20] Shashanka R, Chaira D. Development of nano-structured duplex and ferritic stainless steels by pulverisette planetary milling followed by pressureless sintering. Materials Characterization. 2015;**99**:220-229

[21] Naik HV, e Kalyankar, V.D. Development of NiCrSiBC weld hardfacing approach for P91 steels used in steam turbine componentes. Soldagem & Inspeção. 2021;**26**:1-15

[22] Silva LJ et al. Effect of microstructure on wear performance of NiCrSiBC coatings. Wear. 2019;**428-429**:387-394

[23] Kesavan D, Kamaraj M. The microstructure and high temperature wear performance of a nickel base hardfaced coating. Surface & Coatings Technology. 2010;**204**:4034-4043

[24] Chen X et al. Microstructural evolution of NiCrBSi coatings fabricated by stationary local induction cladding. Journal of Materials Engineering and Performance. 2018;**27**(5):2446-2456